AIAA SciTech Forum
8–12 January 2018, Kissimmee, Florida
2018 AIAA Aerospace Sciences Meeting

10.2514/6.2018-0011

Pylon Design for a Short Range Transport Aircraft with Over-the-Wing Mounted UHBR Engines

L. Savoni[1] and R. Rudnik[2]
DLR, German Aerospace Center, Braunschweig, Germany, 38108

Over-the-wing mounted (OWM) engines, together with their design challenges and their potential in terms of aerodynamic benefits and positive installation effects, are investigated with CFD methods. The analysed reference configuration is a new concept of a civil transport aircraft with short take-off and landing characteristics featuring a circulation control supported high lift system. The concept is intended to provide extraordinary airfield performance while meeting low noise standards. The reference aircraft will be firstly analysed in its wing/body layout. Successively, engine and pylon will be integrated and analysed. A description of the pylon design and parametrization will be given. The results of the wing/body/engine/pylon configuration computations will be discussed in order to assess the transonic flow phenomena taking place on the upper wing when an engine is integrated over the wing in cruise condition and the overall impact of the pylon on the flowfield. Particular attention will be reserved to the flow on the pylon, in order to identify aerodynamic characterisitscs, possible flow separations and to evaluate a strategy for an optimization process. The pylon optimization procedure will be described in detail, together with the tools used and the parameters defining the pylon shape. The preliminary results and trends of the Design of Experiment will eventually be discussed in order to provide an outlook on complete optimization scenarios for such configurations.

I. Introduction

THE worldwide passenger traffic, according to a report by Airbus[1], is expected to double in the next fifteen years. To answer the need of increasing the number of connections, it is necessary to make operational those airports which are currently not usable due to their small size or their proximity to residential areas. However, the modern aviation, in the last decades, is making considerable efforts to become more sustainable and therefore it has to fulfill increasing requirements in terms of low fuel consumption and low noise emissions.

The collaboration between the German Aerospace Center (DLR), the Technical University of Braunschweig and the Leibnitz University of Hannover generated the Collaborative Research Center (Sonderforschungsbereich) SFB 880 which aims, on a long term, to answer the previously discussed needs by investigating technologies and concepts for a low noise transport aircraft with short take-off and landing (STOL) capabilities. STOL characteristics are essential in order to incorporate small sized airports. In fact, as stated in previous studies[2], the capability of taking off and landing on 800 m runways would double the point-to-point connections with respect to the present situation.

The SFB 880 explores two dirrefent engine/airframe integration concepts: a pylon-mounted configuration and an embedded configuration, with the engine partly integrated in the wing structure. In this paper, only the pylon mounted configuration will be analyzed with CFD methods and compared to the reference wing/body (WB) configuration. Detailed information about the pylon design and integration criteria will be given, with a particular focus on the criticalities related to the large pylon size and to its parametrization which is essential for the successive optimization procedure. The ongoing Design of Experiment (DoE) phase is considered as a first phase of the optimization procedure and it will be described in depth and some derived trends will be analyzed, in order to provide an overview on the potential improvement of the pylon design and to assess the challenges of the

[1] Research Scientist, DLR, Institute of Aerodynamics and Flow Technology, Lilienthalplatz 7, 38108, Braunschweig, Germany.
[2] Head of Transport Aircraft Department, DLR, Institute of Aerodynamics and Flow Technology, Lilienthalplatz 7, 38108, Braunschweig, Germany.

aerodynamic integration of such a large component on and over-the-wing mounted (OWM) engines aircraft configuration.

II. Reference configuration

The reference configuration, designated internally as REF3, was designed according to the Technical Data Sheet[3]. Generated as part of the studies in the CRC 880. It is a novel concept of 100-passengers aircraft designed for short distance flights, with a T-tail and a low wing, with ultra-high bypass ratio (UHBR) turbofan engines mounted over the wing, aft of the trailing edge and with the main landing gears stowed in pylon fairings underneath the engines. The wing reference area is 99 m^2 with a span of 28.745 m and a sweep angle of 26°. The reference configuration is depicted in Figure 1.

Figure 1: SFB 880 REF3 configuration[4].

The installation of an engine over the wing is not only beneficial in terms of short take-off and landing potential, but it can offer a broad set of advantages, such as noise reduction due to the shielding of the fan noise offered by the wing´s surface and by the pylon presence itself, reduced weight and length of the main landing gear and reduced risk of foreign object damage during ground operations. However, the design and component implementation of such configurations can be very challenging and lead to a deterioration of the aerodynamic performances, due to the possible increase of the overall installation drag with respect to the conventional under-the-wing mounted (UWM) engines. Previous studies[5] have revealed that OW installations can also lead to an improvement of the aerodynamic characteristics thanks to the favorable installation drag deriving from specific layouts, convenient engine positioning and specific design features.

The present work aims to offer the first results of some investigations on the REF3 configuration in cruise conditions, in order to assess the physical phenomena taking place on the wing, the extent and interference in the transonic regions and the potential in reduction of the installation drag. The aerodynamics of the wing/body (WB) configuration will be briefly introduced and used as a reference in the discussion of the studies presented in the following. The results of the wing/body/engine/pylon (WBEP) configuration will successively be presented, in order to evaluate the impact of the engine and the pylon integration on the flow field. The pylon is in fact expected to have a large influence, due to its large size caused by the necessity of housing the main landing gear. In contrast to more conventional configurations with the main landing gear sowed in the main landing gear bay in the fuselage, the REF3 configuration can do without a large belly fairing. An appropriately designed side of body fairing serves as junction between wing and fuselage while the large pylon fairings host the landing gears. This layout is expected to contribute to the STOL characteristics of the aircraft.

III. Geometry, Numerical Set-Up and Test Case

The geometry representation of the REF3 configuration has been designed according to the prescribed data of the overall design activity[3] by using the commercial software CATIA V5. An ultra high bypass turbofan engine designed by the Institute of Jet Propulsion and Turbomachinery (IFAS) of the Technical University of Braunschweig has been integrated on the WB geometry in the reference position at the spanwise station $\eta = 0.31$. As demonstrated in the study of Hooker[5] and confirmed in the engine position variation analysis carried out on REF3[4,6], this spanwise position is the most beneficial in cruise conditions in terms of interference effects between high speed wing flow and low speed engine flow. In the following phase, the pylon has been designed and adapted to the nacelle and wing geometry.

The pylon design has been one the most challenging tasks of the CAD modelling procedure, due to its large overall encumber deriving from the already mentioned necessity of housing the main landing gear bay. Since no prescriptions except for the dimensions of the cross-sections and of the landing gear bay were provided by the project technical data[3], the pylon shape was arbitrary constructed, taking into account some best practice guidelines and principles present in literature[7]: in general, for wing mounted pylons, the loads have to be distributed in such a manner that the wing deformations are minimized.

The aerodynamic pylon design has been realized following some intuitive principles: the pylon had to respect the prescribed sizes[3] and it had to be aligned with the local flowfield and with smooth intersections with the wing and the nacelle contours. Very small geometrical features have been avoided where possible in order to ease the mesh generation process. The pylon geometry is shown in Figure 2. Some of the geometric characteristics of the pylon are summarized in Table 1.

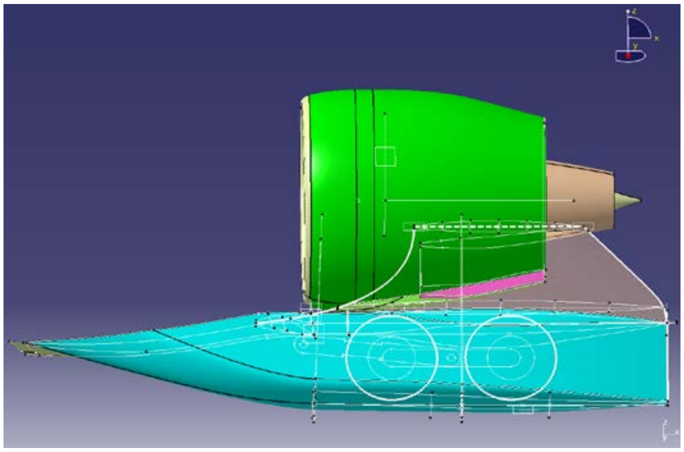

Figure 2: Detail of the construction of the pylon geometry.

Pylon Bottom Thickness	700 mm
Pylon Upper Thickness	338 mm
Pylon Length	3773 mm

Table 1: Geometric characteristics of the pylon.

In this phase of the project, the WBEP configuration has been computed in cruise condition. The corresponding design Mach munber is Ma = 0.78, the cruising altitude is 11,277 m and the target $C_L = 0.46$.

In the perspective of setting up and carrying out an optimization procedure for the pylon shape, the geometrical characteristics of the configuration have to follow the values of the corresponding parameters accordingly. This makes the geometry fully parametric and ready for any future shape optimization process.

To save computational resources, all the studies were carried out on the aircraft´s half geometry, with no tailplanes.

A. Computational grids

The computational grids have been realized by using the commercial software CENTAUR[8]. All the grids are hybrid, due to the higher aptitude of hybrid grids in describing complex 3D flows especially in transonic regime[9].Therefore, the grids consist mainly of prisms and tetrahedras, with structured hexahedras used only to discretize the trailing edges of wing and nacelle and the smallest geometrical features. Smooth intersections between pylon, wing and nacelle surfaces have been established in order to avoid excessive chopping of the prismatic layers and obtain high quality grids.

In order to ensure that the results were sufficiently independent on the grid resolution, a sensitivity study to the grid level of refinement has been conducted. Three families of grids corresponding to three different levels of refinement of the grid (medium, fine, extra-fine) have been tested with the same numerical settings, revealing that the results of the flow simulations were sufficiently grid resolution independent. With the aim of reducing the computational time while still being able to properly resolve small flow features, the medium grids were chosen to proceed with the analysis.

The final WB grid has around 9 Mio. nodes, while the reference WBEP grid has around 22 Mio. nodes. All the grids have a non-dimensional first wall spacing y^+~1 and around 33 prisms layers to capture the boundary layer physics. The surface grid on the wing region is depicted in Figure 3a, while the entire mesh is shown in Figure 3b.

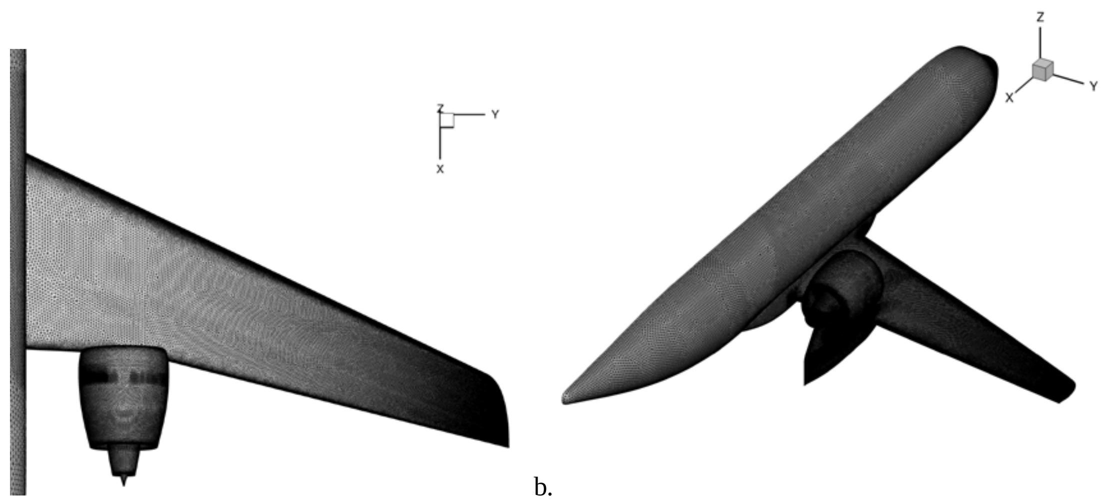

a. b.

Figure 3: Detail of the surface grid on wing and engine (a)[4] and full WBEP grid (b).

In the meshing process, particular attention has been paid to the discretization of the engine inflow and outflow planes. High resolution and uniformity of the mesh in these regions are crucial to properly resolve the engine flow and correctly apply the flow solver´s inlet/outlet planes boundary conditions.

Another important aspect that has been taken into account when producing the grids is the comparability. All the grids generated in the work described in the present paper are generated using the same type and geometry of the grid sources to locally refine the mesh. The driving idea in the optimization process is that the sources are simply repositioned to adapt to the geometric changes, but the number and type of sources and the size of the elements stay the same, in order to preserve comparability between the different flow solutions.

B. Numerical settings

The analysis described in the present paper has been conducted with the DLR TAU-Code by solving the 3D steady Reynolds Averaged Navier-Stokes (RANS) equations with a finite volume method. The flow solver was used in a cell-centered mode. The spatial discretization was accomplished with a central scheme with high matrix dissipation, which proved to be ideal to model complex transonic flow features. Time discretization was completed with the Backward-Euler implicit algorithm. The Spalart-Allmaras turbulence model in its negative formulation described in the flow solver manual and in the work of Blazek [9,10] was employed for all the simulations.

For the high speed simulations, the start of cruise test case was computed, with a Ma = 0.78 and a target C_L=0.46. Therefore, the angle of attack has been varying during the simulations in order to deliver the prescribed lift coefficient.

IV. Results for the baseline configuration

The first results to be shown are the ones related to the WB configuration. The WB computation is crucial to understand the basic aerodynamics of REF3 configuration. The computation at constant lift coefficient reveals a strong shock located at 75% local chord, as shown in Figure 4(b) depicting the pressure diagram at the engine expected spanwise location η = 0.31. Figure 4(a) clearly shows the large extent of the transonic area on the upper wing surface: the mitigation of the shock related wave drag is essential to yield a positive effect of the engine installation on the overall drag, as shown in previous investigations[4]. Furthermore, a trailing edge flow separation at the kink has been detected, extending around 25% span. The resulting angle of attack for the WB configuration at constant lift coefficient is 2.4°. The results of this first simulation have been used as a reference for the following studies.

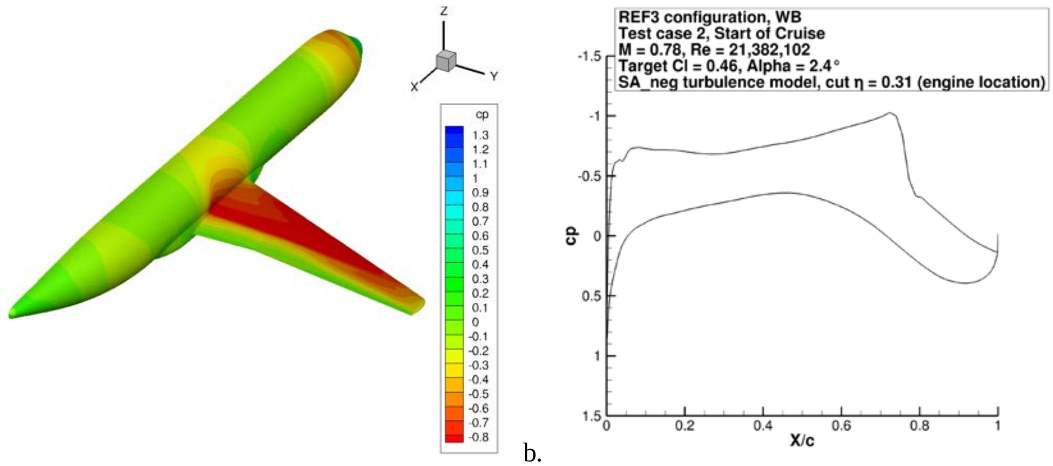

a. b.

Figure 4: Isobars on the surface of the WB configuration (a) and Pressure diagram for the WB at the engine expected location η = 0.31 (b). [4]

In a successive phase, the engine has been integrated in the reference spanwise position η = 0.31, first without any pylon, in order to investigate the effects due to the installation of the engine only, and then with the pylon. The results of the computation of the WBE configuration without pylon have been described in other studies[8] and will be omitted for the sake of brevity. The related pressure diagrams will be shown and briefly discussed in the following paragraphs (Figure 6). One of the main effects due to the engine integration is the reattachment of the flow at the wing´s trailing edge in the proximity of the region where the engine is installed, due to the acceleration of the flow in the gap between the nacelle lower lip and the wing upper surface. The second effect of the integration is the significant increase of the resulting angle of attack at target C_L. When a free-flying engine is implemented on the WB geometry, the resulting angle of attack is around 3.7°.

When the pylon has been integrated in the geometry, the first noticeable consequence has been the decrease of the resulting angle of attack at constant lift by around 1°. The WBEP angle of attack is 2.9°, a more usual value for a cruise condition.

All the other effects of the pylon integration and the differences with respect to the integration of the engine only, can be observed in the following figures. Figure 5 depicts the skin friction lines on the aircraft´s surface drawn on the pressure contour for this initial configuration and engine position. A shock induced separation can be seen on the outboard part of the nacelle, while a pronounced double shock is visible on the outboard wing upper surface. Furthermore, the flow shows a tendency to separate at the trailing edge of the wing in the close proximity of the pylon.

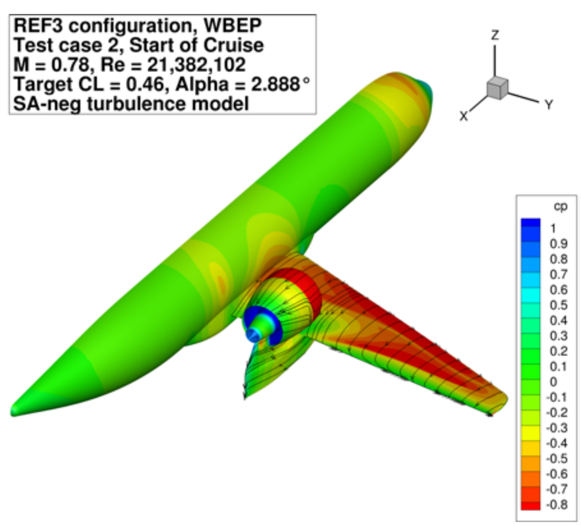

Figure 5: Isobars and skin friction lines on the WBEP surface[6].

Figure 6 depicts the pressure diagrams at two representative wing sections: the proximity of the engine (engine inboard) at η = 0.27 and one outboard section at η = 0.66. In the diagrams, the pressure plots for WB, WBE configuration with free-flying engine and WBEP configuration are shown. From the pressure diagram at the inboard section (Figure 6a), the suction peak for the WBEP configuration is lower, while the shock in the region where the engine is installed is weaker and shifted upstream. The outboard section pressure diagram (Figure 6b) for both WBE and WBEP configuration shows the double shock. When the pylon is integrated, the second shock front is affected since it is moving downstream, probably causing a tendency of the flow to separate at the trailing edge of the wing.

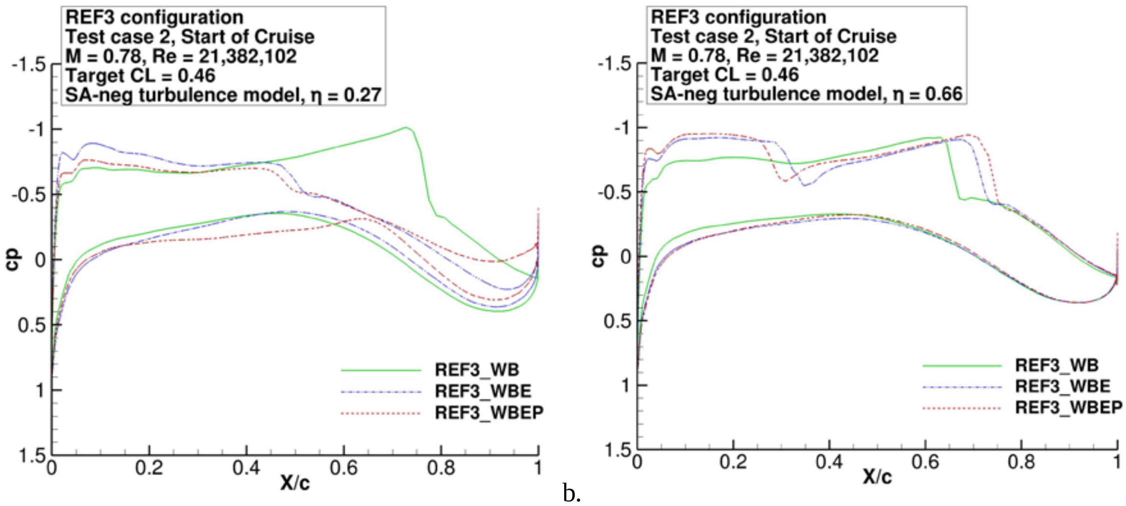

a. b.

Figure 6: Pressure diagrams comparison on WB, WBE and WBEP configuration.

The different configurations have to be evaluated in terms of drag. The DLR in-house tool AeroForce[11] has been used to perform a thrust/drag bookkeeping. In fact, in order to properly investigate the benefits deriving from unconventional engine installations, the values of drag generated by the different airframe components must be recognized and decoupled from the propulsion effects. AeroForce is designed to analyze the aerodynamic forces acting on complex aircraft configurations and it gives the possibility to evaluate the contributions of each single aircraft component to the overall forces. The inputs of the tool are the surface pressure distribution, the velocity and skin friction profiles[11]. AeroForce returns as an output the values of the overall forces, the corresponding forces coefficients and their splitting according to the different components of the analysed geometry.

According e.g. to the procedure described by Hooker et al.[5], the propulsion surfaces have been distinguished from the aerodynamic surfaces. The propulsion thrust is considered to be the contribution of the surface of the engine which are inside the engine streamtube (inlet duct, core cowl, plug, inlet and outlet faces). The aerodynamic drag is the force acting on the outer nacelle cowl up to the inlet highlight. The inner part (inside of the cowl) and aft of the stagnation line is still considered a propulsion surface[5].This bookkeeping procedure allows to have the correct values for thrust and drag coefficients.

The values of the drag components of the WB, WBE with free-flying engine and WBEP configurations will be illustrated in Table 2. The negative values of drag indicate a “positive” contribution to the overall drag, therefore the capability of a component to generate thrust and subsequently reduce the total drag. All the values are expressed in drag counts.

	Body	Nacelle	Wing	Pylon	Overall
WB	91.48	-	159.2	-	250.7
WBE	100.78	-34.91	142.11	-	273.34
WBEP	88.38	-21.68	191.98	24.29	315

Table 2: Results of thrust/drag bookkeeping

The values in the table clearly show that, when integrating additional components on the airframe, the overall drag is increasing as expected. However, the contributions to drag of the single components change considerably and this can be considered as a result of the interference effect of the wing flowfield with the engine flow and the flow over the pylon. The nacelle outer cowling has a positive contribution to the overall drag and this contribution remains positive (but reduced in value) when the pylon is installed. The wing drag, instead, is decreasing with respect to the WB only configuration when an engine is installed over the wing of REF3 configuration. Due to the interaction between the low speed engine flow and the high speed wing flow, as shown in Figure 7 depicting the isobars on the wing surface for the WB and WBE configurations, the shock strength is dramatically reduced and the shock is shifted upstream in the region where the engine is installed. This is the main reason for the observable mitigation of the wing drag. When the pylon is installed, the wing drag is considerably increasing: this might be due to a combination of phenomena, like the strong shock and the consequent shock induced separation originating on the nacelle (Figure 8), the small separation on the pylon (Figure 9) and the absence of the gap between lower lip of the engine and wing surface, which was essential for the flow acceleration an the suppression of the trailing edge separation in that area of the wing[6].

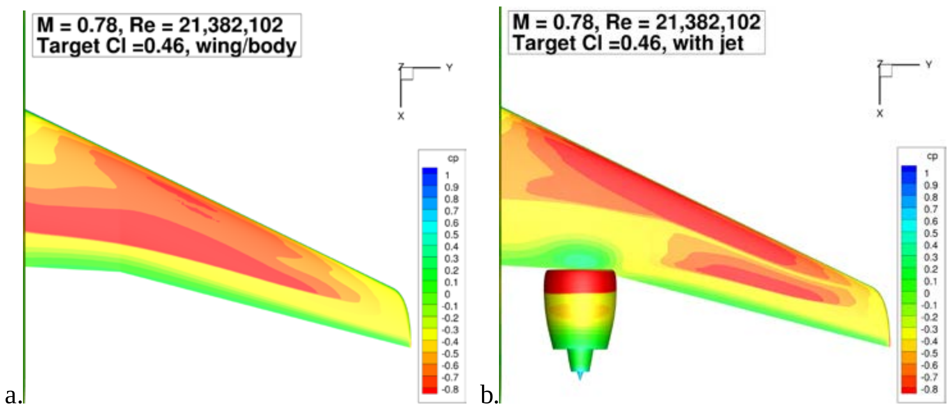

Figure 7: Isobars on the wing for WB (a) and WBE (b).[4]

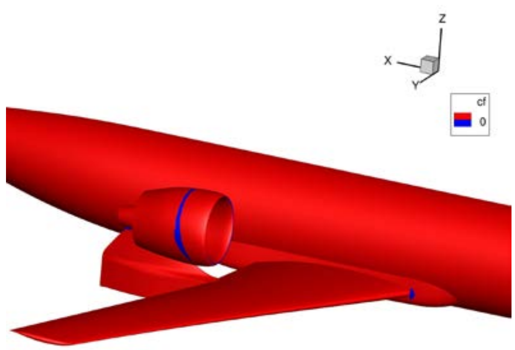

Figure 8: Separation areas on the WBEP.

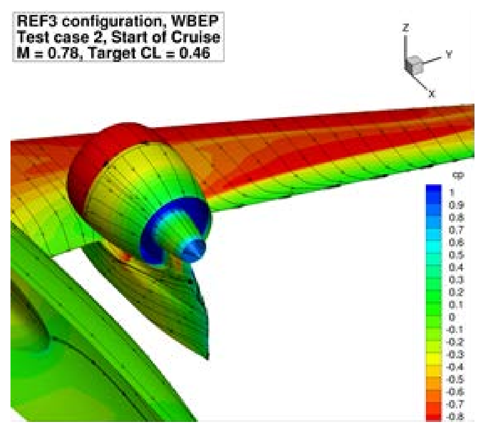

Figure 9: Separation on the pylon.

The value of the overall drag for the baseline WBEP configuration is confirmed by the decomposition of drag into physical components carried out by using the farfield drag extraction tool FFD72 by ONERA. This tool allows a different decomposition of drag with respect to the one seen so far, and more specifically a definition of viscous, induced and wave drag as explained in deep detail in the work of van der Vooren and Destarac[12]. In the case of REF3, the value of the overall drag obtained with FFD72 (319 dcts) is in very good agreement with the one obtained with AeroForce (315 dcts). In particular, REF3 shows a high value of wave drag (38 dcts) probably mainly originating on the nacelle and due to the observable double shock.

Therefore, there is a potential of exploiting the aerodynamic interference effects between engine end elements of the airframe and making OW engine mountings competitive, in terms of performances, with conventional under-the-wing (UW) engines configurations. In this context, the pylon design and optimization might be the key for the modification of the flow on the wing upper surface and the mitigation of drag by trying to improve the wing flowfield.

V. Optimization Set-Up and Preliminary Results

The optimization of the pylon shape is still on-going, but its set-up and preliminary results will be discussed in this paper in order to give an overview of what can be done in the framework of an optimization of one of the most crucial parts of this STOL low noise aircraft concept. One of the fundamental aspects of the set-up has been the pylon parametrization in preparation to the optimization procedure. In the following sections, the choice of the parameters controlling the pylon shape will be described into detail, together with the tools and the settings for the preliminary phase of the optimization and its future steps and objectives.

C. Optimization process

The optimization will be run with the in-house tool PoT SuMo (Powerful Optimization Tools with Surrogate Modelling) described in the work of Wilke[13]. The surrogate model based optimization has been chosen since it can be considered as an accelerated version of a conventional optimization. Based on an abstraction of the true mathematical function, the code creates a surrogate model simulating the design space. The biggest advantage resides in the fact that the surrogate model is quicker to evaluate. The biggest disadvantage is the lack of accuracy with respect to more ordinary methods, which can however be compensated by refinining the region of interest through parameters.

To perform the full optimization procedure, firstly a Design of Experiment (DoE) needs to be performed. In this phase, the samples to build our design space are selected. To be as accurate as possible, the number of samples needs to be at least ten times the number of the parameters involved in the optimization. The sampling has been done with a Latin Hypercube with the use of Central Vonoi tessellation[13] to distribute in an even pattern the samples in the design space. After this phase, the surrogate model is built and it can be improved in the regions of interest through parameters. The surrogate model must be efficient and robust with respect to the analysed aerodynamic problem. The regions of no interest must be indicated as well, therefore a good optimization algorithm must be chosen to indentify the in-fill point. This in-fill criterion identifies new samples to improve the selected surrogate model, in an iterative process that proceeds until the design confidence is met or a certain convergence is reached and the optimum is found.

In the specific case of this work, the procedure of the optimization has been coupled to the geometry update, to the mesh generation and to the CFD computations in a fully automatic process.

D. Pylon Parametrization

The design of the geometry of the pylon has been a crucial point of the work described in this paper, due to the structural importance of this component and to the previously discussed necessity of allocating the main landing gear bay in the under-pylon fairing. Moreover, the pylon fairing itself can have an important role in shielding, together with the wing, part of the noise coming from the engine jet. All these important aspects have been taken into account in the design phase and in the successive selection of the parameters for the shape optimization process. As a result, the pylon was severely constrained by design prescriptions. In the selection of the eight parameters to adopt in the shape optimization process, the following design driving principles and constraints have all been considered and they will be described in the next paragraphs.

As a first prescription, the lower fairing thickness (parameter 1) could only be increased for structural reasons. According to the data sheet of the overall design activity[3], the lower thickness must be between 700 mm and 800 mm and these sizes have been considered as upper and lower boundaries for this first parameter.

The other sections of the pylon were constrained due to the fact that the pylon has to contain some essential systems and wirings. The only section which could be modified in thickess was the most upper section (light blue) in Figure 10 and its thickness had to be between 300 mm and 400 mm (parameter 2).

In previous studies, the increase of pylon length has proven to be beneficial in terms of aerodynamic performances, since the aerodynamic interference effects can be minimized by optimally contouring nacelle, pylon and fairings and therefore superimposing the kind of flow around such bodies[15]. Subsequently, the pylon length has been considered as another parameter of the optimization process (parameter 3). The pylon length could be also slightly decreased compatibly with the landing gear bay, but keeping in mind the pylon role in the noise shielding. In order to avoid the possibility that the pylon touched ground in take-off or landing, the increment of its length must be maximum 500 mm beyond the prescribed length.

Taking the constraints on the upper pylon thickness into account, the upper shape could be anyway modified. To modify the shape of the upper section, the normals to the chord of the respective airfoil have been used and scaled. These values to scale the length of the normals are the final five parameters of the optimization process.

In total, the parameters for the shape optimization are eight.

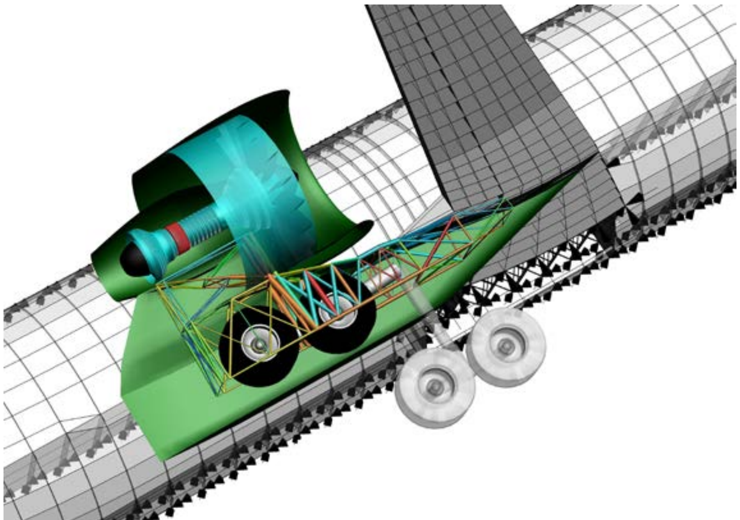

Figure 10: Pylon constraints[14].

E. Automatic procedure

After the parameters are chosen, the objective function is selected. In the present case, the objective function is the drag coefficient. At this point, the automatic DoE procedure starts.

At the end of each iteration of the DoE, a sample corresponding to new values of the parameters is selected. The geometry is updated and successively a new mesh with the same numerical settings is generated. The new configuration is then evaluated with CFD methods and the aerodynamic coefficients from TAU are evaluated with AeroForce. Since the pylon is intersecting the engine geometry, effects of the values of thrust and drag are expected when varying the pylon shape, therefore it is fundamental to have a thrust/drag bookkeeping to complete the assessment in order to evaluate the correct values of thrust and drag and find an optimum corresponding to the real minimum drag. When the AeroForce evaluation is completed, a new iteration starts until the sampling is completed.

The DoE for the pylon shape is still in progress but some trends can be observed and they will be discussed in the following section. At the end of the DoE phase, the Differential Evolutionary (DE) algorithm[13] will be chosen to drive the members of the initial population towards the Pareto front. Evolutionary algorithms present less risk to run into a local optimum and the high computational cost of this method can be tolerated in this case, since the number of parameters involved in the optimization is not too large.

F. DoE Preliminary Results

The preliminary results of a first phase of the DoE will be presented in this section of the paper.

An increase in pylon length results in an increase in the final angle of attack at target lift coefficient. Due to the presence of the engine over the wing and to the highly twisted wing[3] of the baseline configuration, high angles of attack have been observed in all the previous studies[4,6]. More specifically, considering the same target lift coefficient equal to 0.46, the resulting angle of attack is 2.4° for the WB, 3.8° for the WBE with free-flying engine and 2.9° for the WBEP in the reference configuration. The values of the resulting angles of attack observed so far in the DoE are all between 3.5° and 3.9°, but this is not a crucial downside since it could improve the attitude of the aircraft in landing configuration.

The configuration that has revealed the minimum value of overall drag in the first half of the DoE is corresponding to very small modifications on the upper and lower sections thicknesses of the pylon but to an increase of the pylon length by around 164 mm. This configuration is compared to the baseline in Table 3.

	Bottom thickness [mm]	Upper thickness [mm]	Length [mm]	AoA	Overall drag [dcts]
WBEP REF3	700	338	3773	2.888°	315
WBEP DoE	700.782	324.840	3936.666	3.851°	311

Table 3: Configurations comparison.

The observed reduction in drag is by less than 2% with respect to the baseline configuration, since the two configurations are really similar. Some differences in the installation effects can however be seen. As observable in Table 4, the overall positive contribution given by the nacelle outer cowling is considerably decreasing with respect to the baseline. The drag generated by the pylon is higher, probably due to the increase in length. However, the drag of the wing is much lower for the optimum candidate and that´s the main reason for the observable drag decrease.

	Nacelle	Wing	Pylon	Overall
WBEP REF3	-21.68	191.98	24.29	315
WBEP DoE	-12.58	169.59	28.49	311

Table 4: Thrust/Drag bookkeeping comparison [dcts].

In terms of overall flow on the wing upper surface, for the best result deriving from the preliminary DoE, the first transonic area seems to be slightly more extended while the second seems to be less extended compared to the WBEP baseline reference configuration (Figure 11) and the flow is considerably decelerating at the engine highlight. Another important consequence is that the pylon modifications suggested by the DoE indicate a considerable reduction of the shock induced separation on the nacelle (Figure 12). This can contribute to the mitigation of the overall drag. However, these results are still preliminary and more relevant improvements can be expected from the complete DoE and then from the full optimization procedure.

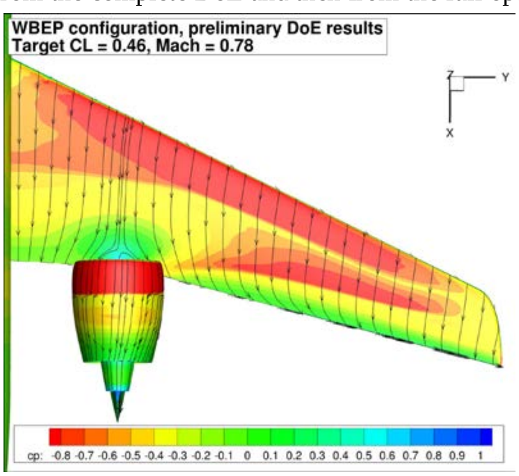

Figure 11: Skin friction on pressure contour.

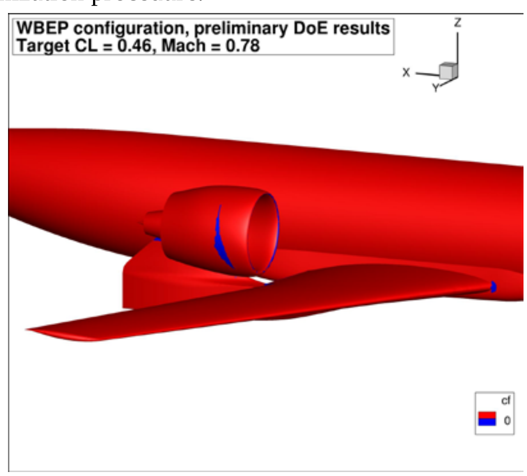

Figure 12: Separation areas on the DoE result.

VI. Conclusion

An assessment of over-the-wing pylon mounted engine installations has been provided in this abstract for a STOL short range aircraft concept. 3D RANS equations have been solved to evaluate the wing/body configuration, the effects of the installation of a UHBR turbofan engine and pylon over the wing. Isobars and pressure diagrams of the configurations were evaluated. As a result of this analysis, the pylon has proved to have a significant impact on the resulting flow field: integrating the pylon can lead to a desirable reduction of the cruise angle of attack but the outboard flow still has significant potential for improvement, for instance by means of distinct wing shape optimization. A first optimization is being carried out at present for the pylon. The preliminary assessment of the DoE phase indicates a potential in drag reduction which still needs to be deeply investigated. Therefore, in a successive phase, a nacelle shape optimization will be performed, in order to suppress the observed shock induced separation on the nacelle cowling. Both, the double shock on the wing upper surface and the shock induced separation on the outer nacelle are definitely installation related phenomena, therefore the shape optimization can be the key for the improvement of the flowfield in the outboard part of the wing and the mitigation of the wave drag, that will be evaluated for the selected configuration with a farfield drag decomposition method. The long term aim of the project is to demonstrate that over-the-wing nacelle installation have a high potential of aerodynamic improvement with respect to the conventional under-the-wing engines layouts for the present aircraft concept. This is to be accomplished by properly modifying the airframe shape taking all relevant components, wing, pylon and nacelle, into account and exploiting the interference between the different components. The cruise efficient configuration will be then validated in low speed with full high lift systems and active flow control implemented, to verify the compliance with the STOL requirements.

Acknowledgments

Financial support has been provided by the German Research Foundation (Deutsche Foschungsgemeinschaft – DFG) in the framework of the Sonderforschungsbereich 880. In the design of the geometry of the reference configuration and in the solution of many technical issues, Arno Ronzheimer from the Transport Aircrafts department of DLR Braunschweig gave a fundamental and really valuable support. The authors want to acknowledge Fabian Lange and Guther Wilke for the support given in the optimization procedure.

References

[1]Airbus S.A.S., "Flying by Numbers, Global Market Forecast 2015-2034", Blagnac, France, 2015, pp. 9.

[2]L. Müller, W. Heinze, D. Kozulovic, M. Hepperle, R. Radespiel, „Aerodynamic Installation Effects of an Over-the-Wing Propeller on a High-Lift Configuration", *Journal of Aircrafts*, Vol. 51, No. 1, 2014, pp. 249.

[3]W. Heinze, T. Weiss, "Main Data Sheet. A/C Type: SFB 880 Reference Aircraft REF3-2015", 2015.

[4]L. Savoni, R. Rudnik, "Aerodynamic Assessment of Pylon-Mounted Over-the-Wing Nacelle Installations on a STOL Commercial Aircraft Concept", on "New Results on Numerical and Experimental Fluid Mechanics", SPRINGER, 2016.

[5]J. Hooker, A. Wick, C. Zeune, A. Agelastos, "Over-the-Wing Nacelles Installations for Improved Energy Efficiency", 31st AIAA Applied Aerodynamics Conference, San Diego, CA, 2013.

[6]L.Savoni, C. Heykena, R. Rudnik, J. Friedrichs, "Aerodynamic Analysis of Rear Mounted Over-the-Wing Turbofan Engines for Cruise Conditions", Sonderforschugsbereich 880 Biennial Report, 2017.

[7]M. Chung-Yung Niu, "Airframe Structural Design: Practical Design Information and Data on Aircraft Structures", Lockheed Aeronautical Systems Company, California, Chapter 13.

[8]CentaurSoft Homepage, www.centaursoft.com.

[9]J. Blazek, "Computational Fluid Dynamics: Principles and Applications", ELSEVIER, 2001.

[10]TAU-Code Users Guide, Release 2015.1.0, 2015.

[11]J. Wild, "AeroForce Aerodynami Force Analyzer" version 0.4, User manual, 1999.

[12]J. van der Vooren, D. Destarac, „Drag/thrust analysis of jet propelled transonic transport aircraft: Definition of physical drag components", in „Aerospace Science and Technology", ELSEVIER, 2004.

[13]G. Wilke, "Powerful Optimization Tools with Surrogate Modelling.User and Developer´s Manual", 2015.

[14]Niu, Michael C.Y.: "Airframe Structural Design: Practical Design Information and Data on Aircraft Structures," 611 pages, published by Hong Kong Commilit Press Ltd., ISBN-962-7128-04-X, January 1991, chapter 13.9 engine mounts, section loads, pp.474.

[15]M. Fujino, "Case Study 4: Honda Jet", American Institute of Aeronautic and Astronautics, pp. 615-647.